Open access • Journal Article • DOI:10.1038/MP.2017.171

Tau-mediated iron export prevents ferroptotic damage after ischemic stroke

Qing-Zhang Tuo, Qing-Zhang Tuo, Qing-Zhang Tuo, Peng Lei ...+19 more authors

Institutions: Sichuan University, Florey Institute of Neuroscience and Mental Health, Huazhong University of Science and Technology, University of Melbourne

Published on: 08 Sep 2017 - Molecular Psychiatry (Nature Publishing Group)

Topics: Brain ischemia, Artery occlusion, Reperfusion injury and Stroke

Molecular Psychiatry (2017) 00, 1–11

www.nature.com/mp

IMMEDIATE COMMUNICATION

Tau-mediated iron export prevents ferroptotic damage after ischemic stroke

Q-z Tuo[1,2,3,7], P Lei[2,3,7], KA Jackman[2,7], X-l Li[3], H Xiong[3], X-l Li[2,4], Z-y Liuyang[1], L Roisman[5], S-t Zhang[3], S Ayton[2], Q Wang[3], PJ Crouch[5], K Ganio[2], X-c Wang[1], L Pei[6], PA Adlard[2], Y-m Lu[1], R Cappai[5], J-z Wang[1], R Liu[1] and AI Bush[2]

Functional failure of tau contributes to age-dependent, iron-mediated neurotoxicity, and as iron accumulates in ischemic stroke tissue, we hypothesized that tau failure may exaggerate ischemia–reperfusion-related toxicity. Indeed, unilateral, transient middle cerebral artery occlusion (MCAO) suppressed hemispheric tau and increased iron levels in young (3-month-old) mice and rats. Wild-type mice were protected by iron-targeted interventions: ceruloplasmin and amyloid precursor protein ectodomain, as well as ferroptosis inhibitors. At this age, tau-knockout mice did not express elevated brain iron and were protected against hemispheric reperfusion injury following MCAO, indicating that tau suppression may prevent ferroptosis. However, the accelerated age-dependent brain iron accumulation that occurs in tau-knockout mice at 12 months of age negated the protective benefit of tau suppression against MCAO-induced focal cerebral ischemia–reperfusion injury. The protective benefit of tau knockout was revived in older mice by iron-targeting interventions. These findings introduce tau–iron interaction as a pleiotropic modulator of ferroptosis and ischemic stroke outcome.

Molecular Psychiatry advance online publication, 8 September 2017; doi:10.1038/mp.2017.171

INTRODUCTION

Stroke is a leading cause of death and major cause of permanent disability, with a 40% mortality within 12 months and 50% becoming permanently dependent.[1] Acute ischemic stroke is the most common form of stroke (accounting for ~85% of total stroke cases) and occurs as a result of vascular occlusion.[2] Clinically, treatment for stroke is limited to interventions that restore blood flow—either pharmacologically or via mechanical thrombolysis. However, in practice only 11% of stroke patients actually receive tissue-type plasminogen activator, and of those patients, half fail to demonstrate clinical improvement.[3] There is therefore an urgent need to identify new, more effective treatments for ischemia–reperfusion-related neuronal damage.

The pathogenic processes regulating brain injury after stroke have established roles for multiple processes including inflammation, excitotoxicity, oxidative stress and apoptosis.[4] By inhibiting these pathways experimentally, numerous drug candidates and genetic modifications have demonstrated neuroprotection in rodent models of stroke. However, despite the abundance of successful interventions in preclinical stroke, these benefits have failed to translate to the clinic.[5]

Age is a major risk factor for stroke, with >80% of strokes occurring in individuals over 55 years of age.[6] Aged rodents are significantly more vulnerable to sequelae of cerebrovascular occlusion in experimental stroke for reasons that are uncertain.[7,8] Understanding how natural aging increases susceptibility to stroke, and using appropriately aged animal models to study candidate interventions, could increase the potential for translating stroke interventions. We, and others, have shown that the process of natural aging reliably induces the elevation of brain iron in rodents and humans.[9–11] This is important as iron accumulation induces oxidative stress, and ischemic stroke is complicated by iron accumulation in affected regions in human and animal models,[12–16] which exaggerates neuronal damage during reperfusion.[17,18] Iron-fed animals are more susceptible to middle cerebral artery occlusion (MCAO),[19] and iron chelation attenuates ischemic–reperfusion damage in animal models.[20–23] The underlying mechanism of ischemia–reperfusion-induced iron accumulation and its related toxicity remains unclear.

Tau protein, which becomes hyperphosphorylated to form neuronal tangles in tauopathies like Alzheimer's disease and Parkinson's disease,[24] functions to facilitate neuronal iron efflux and therefore loss of normal soluble tau may contribute to neurotoxic iron accumulation in these diseases.[11,25–28] Despite this, tau knockout attenuates the neurodegenerative phenotypes of transgenic mice overexpressing mutant amyloid precursor protein (APP), an aggressive model for Alzheimer's disease.[29–31] The neuroprotective benefits of tau ablation, although appear to be lost with age,[32] indicate that tau may have pleiotropic activities depending on context. We therefore hypothesized that the tau-

[1]Department of Pathophysiology, Key Laboratory of Ministry of Education for Neurological Disorders, School of Basic Medicine, Tongji Medical College, Huazhong University of Science and Technology, Wuhan, China; [2]Oxidation Biology Unit, Florey Institute of Neuroscience and Mental Health, The University of Melbourne, Melbourne, VIC, Australia; [3]Department of Neurology and State Key Laboratory of Biotherapy, West China Hospital, Sichuan University, and Collaborative Innovation Center for Biotherapy, Sichuan, China; [4]Department of Neurology, The Fourth Affiliated Hospital, Harbin Medical University, Harbin, China; [5]Department of Pathology, The University of Melbourne, Melbourne, VIC, Australia and [6]Department of Neurobiology, School of Basic Medicine, Tongji Medical College, Huazhong University of Science and Technology, Hubei, China. Correspondence: Professor P Lei, Department of Neurology and State Key Laboratory of Biotherapy, West China Hospital, Sichuan University, Chengdu 610041, China or Professor R Liu, Department of Pathophysiology, Key Laboratory of Ministry of Education for Neurological Disorders, School of Basic Medicine, Tongji Medical College, Huazhong University of Science and Technology, Wuhan 430030, China or Professor AI Bush, Oxidation Biology Unit, Florey Institute of Neuroscience and Mental Health, The University of Melbourneh, 30 Royal Parade, Parkville, VIC 3052, Australia.
E-mail: peng.lei@scu.edu.cn or rong.liu@hust.edu.cn or ashley.bush@florey.edu.au
[7]These authors contributed equally to this work.
Received 10 April 2017; revised 20 June 2017; accepted 6 July 2017

related iron export pathway might be involved in iron accumulation in ischemic stroke.

MATERIALS AND METHODS

Reagents

Reagents were purchased from Sigma (Sigma-Aldrich, Castle Hill, NSW, Australia; Sigma-Aldrich, Shanghai, China), unless specified.

Mice

All mice were housed in a specific pathogen-free facility according to standard animal care protocols and fed standard laboratory chow (Code 102108, Barastoc, Ridley AgriProducts) and tap water *ad libitum*. All mouse procedures were approved by the Florey Institute animal ethics committee (15-019) or West China hospital of Sichuan University animal ethics committee, and were performed in accordance with the National Health and Medical Research Council guidelines. Mice on a background of sv129 and C57Bl/6[33] were originally obtained from Dr M Vitek (Duke University, Durham, NC, USA) and maintained homozygously, with mutants backcrossed to the parental inbred strain every three generations. The male C57Bl/6 mice (25–30 g) were purchased at 12 weeks of age from the Animal Resources Centre, Western Australia, or from the Institute of Laboratory Animals of Sichuan Academy of Medical Sciences and Sichuan Provincial People's Hospital, China.

Sprague–Dawley rats

Adult (90 ± 5 days old) male Sprague–Dawley rats weighing 250–300 g were housed individually under standard conditions of temperature and humidity, and a 12 h light–dark cycle (lights on at 0800 hours), with free access to food and water before use. Adequate measures were taken to minimize pain or discomfort during surgeries. All rat experiments were carried out in accordance with the Institutional Guidelines of the Animal Care and Use Committee (Huazhong University of Science and Technology, China).

Focal cerebral ischemia model

Transient acute focal cerebral ischemia was induced by intraluminal MCAO, as described previously.[34,35] All animals used in this study are male since female mice are affected by their estrous state, which may compromise the lesion induced by the procedure.[36] Briefly, after weighing, mice were randomly assigned (by Excel 2013) into experimental groups, and then deeply anesthetized with 5% isoflurane in 30% O_2/70% N_2O using the Anesthesia System (Mediquip, Loganholme QLD, Australia). The level of isoflurane was then reduced and maintained at 1%. Rats were anesthetized with intraperitoneal injection of 10 mg kg^{-1} xylazine and 300 mg kg^{-1} chloral hydrate. A 4-mm distal nylon monofilament (30 mm in length, 0.16 mm in diameter; Amber, Kuji, Japan) segment was coated with 0.21–0.22 mm diameter silicone (Henkel, Kilsyth, VIC, Australia) for mice, and an 11-mm distal monofilament (50 mm in length, 0.23 mm in diameter) segment was coated with 0.28–0.30 mm diameter silicone for rats. MCAO was performed by insertion of the monofilament via the common carotid artery into the left internal carotid artery, advanced 9–10 mm (in mice) or 20–21 mm (in rats) past the carotid bifurcation until a slight resistance was felt. Body temperature of the animal was maintained at 37 ± 0.5 °C throughout the procedure using a heat pad. Temperature and respiratory rate were monitored during surgery.

We visualized brain–blood perfusion in real time during the MCAO procedure using a PeriCam PSI System (Perimed, Järfälla, Sweden). The room temperature during the experiment was controlled at 26 ± 1 °C, and relative humidity was maintained 50–60%, with no direct sunlight indoors. The PSI parameters were set as follows: image acquisition rate, 50 HZ; normal resolution, 0.04 mm; 5 frame per second; the working distance is 13 ± 0.5 cm; the monitor area is 1 (highness) × 1 (width) cm^2; the region of interest is 0.5 cm around the Bregma. PIMSoft Software (Stockholm, Sweden) was used for recording, storage and analysis. Perfusion unit was the base unit for blood perfusion. Higher perfusion unit indicated greater blood perfusion. Cerebral blood flow to the MCA territory was measured using a laser Doppler monitor (Moor Instruments, Axminster, UK) by attaching a fiber optic probe to a position 3 mm posterior and 3 mm lateral to the bregma on the surface of the cranium. Common carotid artery occlusion and MCAO values were normalized and expressed as a percentage of baseline cerebral blood flow. Peripheral oxygen saturation and heart rate were monitored by attaching a probe to the left hind paw of the animal and recorded using a PhysioSuite monitoring device (Kent Scientific, Torrington, CT, USA).

The filament was left in place for 60 min in 3-month-old mice (or 45 min in 12-month-old mice, to ensure a satisfactory rate of survival), and 90 min in rats, and then withdrawn for reperfusion. In the sham-operated animals, the occluding filament was inserted only 5 mm above the carotid bifurcation. We excluded mice from further studies if excessive bleeding occurred during surgery, if the operation time exceeded 90 min, if the mouse failed to recover from anesthesia within 15 min or if hemorrhage was found in the brain slices or at the base of the Circle of Willis during post-mortem examination.

Post surgery neurological evaluation

The neurological assessment post surgery was performed by an investigator blinded to the experimental groups, and confirmed by a second investigator blinded to the experimental groups. After 0, 6 and 24 h of MCAO/reperfusion, the neurological deficit of each mouse or rat was evaluated by a five-point scale as described previously:[37] 0, no observable deficit; 1, right forelimb flexion; 2, decreased resistance to left lateral push (and right forelimb flexion) without circling; 3, same behavior as grade 2, with circling to right; 4, severe rotation progressing into barreling, loss of walking or righting reflex.

Rotarod treadmill test

Motor coordination of the animals after operation and treatment was measured using a rotarod treadmill for mice (Ugo Basile, Monvalle, Italy), under the accelerating rotor mode (10 speeds from 4 to 40 r.p.m. for 5 min). The interval from when the animal mounted the rod to when it fell off was recorded as the retention time, and mice that lasted for 300 s on the accelerating rotating rod were recorded as survivors. The animals were trained for 2 days, 3 trials per day, before surgery, and the mean duration on the rod was recorded to obtain stable baseline values. Performance on the rotarod test was measured three times a day in the 4 weeks following the ischemic insult.

Water maze test

One week after MCAO/reperfusion, spatial learning was assessed by Morris water maze test. Mice were trained to find a hidden platform in the water maze (0.8 m diameter) for 5 consecutive days, 4 trials (30 s intervals) per day from 1000 to 1800 hours. For each trial, the mouse started from one of the four quadrants, facing the wall of the pool, and ended when the animal climbed onto the platform. If the mice did not locate the platform within 60 s, they were guided to the platform. The swimming path and the time used to find the platform (latency) or pass through the previous platform quadrant were recorded each day by a video camera fixed to the ceiling, 1.5 m from the water surface. The camera was connected to a digital-tracking device attached to a computer.

Novel objective recognition test

A second memory test, Novel Objective Recognition test, was performed as described previously.[31] Briefly, 24 h before the test, the mice were habituated to the arenas (50 cm × 50 cm plastic

container) for 5 min without objects. The day after the mice re-entered the arenas from the same starting point of the arena (facing the bottom left corner) and granted 10 min to familiarize themselves with the objects (50 ml tubesx2 spaced 10 cm apart). After each familiarization period the arena and objects were cleaned with ethanol. Exactly 1 h after the familiarization period, one of the 50 ml tubes was replaced with a T75 tissue culture flask as the 'Novel' object and the mice were granted 10 min to explore both objects. This recall period was recorded on camera for subsequent blinded analysis by two independent observers.

TTC staining

After 24 h of MCAO/reperfusion, mice were weighed and killed with an overdose of sodium pentobarbitone (Lethabarb, 100 mg kg^{-1}). Rats were weighed and killed with an overdose of 10 mg kg^{-1} xylazine and 1 g kg^{-1} chloral hydrate intraperitoneally. The brain was removed rapidly and placed in − 20 °C for 20 min. Coronal slices were made at 2 mm intervals from the frontal poles, and sections were immersed in 0.5% 2,3,5-tripenyltetrazolium chloride (TTC) in phosphate-buffered saline at 37 °C for 20 min. The presence or absence of infarction was determined by examining TTC-stained sections for the areas on the side of infarction that did not stain with TTC. The brain slices were fixed in 4% paraformaldehyde at 4 °C until imaging.

Quantitative measurement of brain infarct volume

Serial sections were photographed using a digital camera and the area of infarct was quantified with Image J (1.49 m; NIH, Bethesda, MD, USA) by an investigator blinded to the experimental groups. The area of infarct (white, unstained), the area of ipsilateral hemisphere (white, unstained, plus red brick, stained) and the area of the contralateral hemisphere (red brick, stained) were measured for each section by a blinded operator. The volume was calculated by summing the representative areas in all sections and multiplying by the slice thickness, and then correcting for edema, as previously described:[38] corrected infarct volume (CIV) = contralateral hemisphere volume − (ipsilateral hemisphere volume − infarct volume).

Nissl staining

The rats were deeply killed by intraperitoneal injection of chloral hydrate (1 g kg^{-1}) and then fixed by transcardial perfusion with 0.9% NaCl, followed by 4% paraformaldehyde in 100 mM phosphate buffer. After perfusion, the brains were postfixed in the same solution overnight at 4 °C. Coronal sections of the brain were cut (30 μm thick) by Vibratome (Leica Microsystems, Milton Keynes, UK; S100, TPI) and immersed in 1% toluidine blue for 3 min. Sections were then dehydrated using 95 and 100% ethanol solutions, made transparent using xylene, placed under coverslips and analyzed by microscope (Nikon, 90i, Tokyo, Japan). For mouse, paraformaldehyde-fixed frozen sections were air dried for 30 min before staining. The slides were then placed into a slide rack and immersed in 1% Neutral Red for 2 min. The slides were then rinsed, placed into a series of ethanol concentrations starting from 50 to 100% and immersed into xylene two times for 5 min each. The slides were then coverslipped using DPX mounting medium (BDH, Trajan Scientific Australia Pty, Ringwood, VIC, Australia) and air dried. The neurons per x40 magnification in the CA1 area were quantified by an investigator blinded to the experimental group, using Imaging-Pro Plus 6.0 (Media Cybernetics, Rockville, MD, USA).

Expression and purification of recombinant APP695 ectodomain

The APP695 ectodomain (APP695ec) (LEV to GSNK, amino-acid residues 18–624)[39] was cloned into the mammalian expression system pHL-sec with an Fc tag.[40] The APP695ec was transiently expressed in HEK293T cells and the media were collected after 10 days. Purification was carried out by affinity purification with Protein G-Sepharose followed by thrombin cleavage to remove the Fc tag, with a final step of size-exclusion chromatography using Superdex 200. Purity was confirmed by mass spectrometry and sodium dodecyl sulfate-polyacrylamide gel electrophoresis.

Preparation of apo-ceruloplasmin

Ethylene diamine tetraacetic acid disodium salt, dihydrate (EDTA; 0.5 M) was prepared by dissolving in double-distilled water (ddH_2O) and adjusting the pH with NaOH to 8.0. Apo-Cp (30 mg) was prepared by incubation (1 h, 37 °C) with EDTA (0.5 M) and buffer exchanged into ddH_2O by repeated washes in ddH_2O (five times) and finally with saline (0.9% NaCl) through a 30 kDa cutoff Amicon Ultra-15 (Millipore, Billerica, MA, USA) centrifugal filter unit. The remaining Cp was adjusted with saline to a final concentration of 10 mg ml^{-1} and frozen at − 20 °C. Cp (30 mg) control was prepared in the same way in ddH_2O without EDTA. The subsequent flow through was used as the vehicle control.

Drug treatments

The mice or rats were chosen randomly for treatment (by Excel 2013). Cp (5 mg kg^{-1} intraperitoneally, Biofarma, Kyiv, Ukraine) or vehicle (0.9% saline) was injected into mice immediately after MCAO/reperfusion. APP695ec (5 mg kg^{-1}, intravenously), ML351 (20 mg kg^{-1}, intravenously; Sigma, USA) or vehicle (0.9% saline) was injected into the C57Bl/6 mice immediately after MCAO/reperfusion via the caudal vein. Liproxstatin-1 (5 mg kg^{-1}, 10 mg kg^{-1}; Selleckchem, Houston, TX, USA), Ferrostatin-1 (5 mg kg^{-1}, 10 mg kg^{-1}; Sigma, St. Louis, MO, USA) or vehicle (18.8% DMSO in 0.9% saline) were delivered intranasally by pipette to mice immediately after MCAO/reperfusion or 6 h post reperfusion.

Ferroxidase assay

The transferrin loading (Ferric Gain) and the Ferrous Loss ferroxidase assays were conducted as described previously.[41] In 200 μl reaction mixes (final concentrations): sample (500 ng protein per ml) was added to PIPES (200 mM, pH 6.5) in the presence of apo-TF (50 μM). Ferrous ammonium sulfate (100 μM) was used as the substrate for the assay, was dissolved in N_2-purged ddH_2O and added as the last component of the assay to initiate the reaction. For the Ferric Gain assay, absorbance readings (310 and 460 nM) were monitored at 1 min intervals over 10 min at 24 °C with agitation on a microplate spectrophotometer (PowerWave HT; BioTek, Burlington, VT, USA), and the readout at 5 min was reported. For the Ferrous Loss assay, Ferene S (500 μM) was added at the end of 10 min, briefly agitated and absorbance (590 nm) read immediately. Reactions were blanked against sample buffers that had all components in the reaction mix except the sample itself. Extinction coefficients of Fe were 2.28 mM^{-1} Fe^{3+} cm^{-1} for transferrin loading (Ferric Gain) and 37.3 mM^{-1} Fe^{2+} cm^{-1} for Ferrous Loss assays.

Mouse sample preparation and western blot

After reperfusion at 0, 0.5, 1, 3, 6 and 24 h, mice were deeply anesthetized and transcardial perfusion with phosphate-buffered saline was performed before the brains were removed. Hippocampi were dissected and homogenized in ice-cold lysis buffer containing 50 mM Tris-HCl (pH 7.6), 150 mM NaCl, 1% (v v^{-1}) Triton X-100, EDTA-free protease inhibitor cocktail (1:50; Roche, Dee Why, NSW, Australia) and phosphatase inhibitors II and III (1:1000). Total protein concentration was determined by the BCA protein assay (Pierce, Mt Waverley, VIC, Australia). Aliquots of homogenate with equal protein concentrations were separated in 4–12% Bis-Tris gels with NuPAGE MES running buffer (Invitrogen, Carlsbad, CA, USA), and transferred to nitrocellulose membranes by iBlot2 (Invitrogen). The membranes were blocked with milk (10% (v v^{-1})) and probed with appropriate primary and secondary IgG-HRP-conjugated antibodies (Dako, Glostrup, Denmark). Enhanced chemiluminescence detection system (GE Healthcare, Little

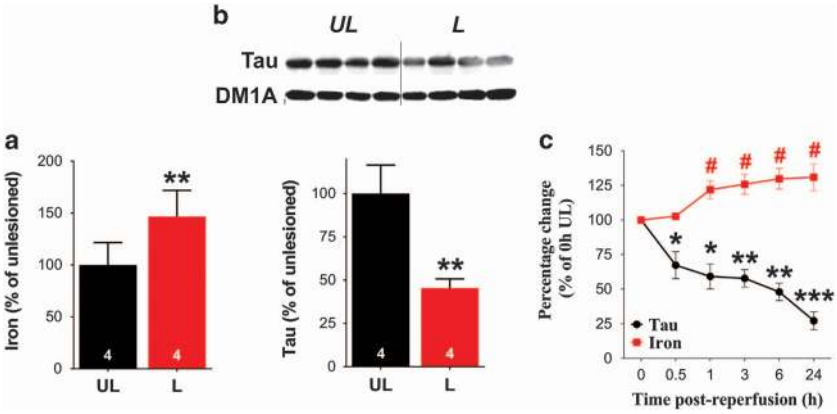

Figure 1. Tau protein in focal transient ischemia. (**a**) Cortical iron levels in rat 6 h after MCAO/reperfusion comparing lesioned (L) to unlesioned (UL) hemispheres, normalized to tissue wet weight. Data are means ± s.e.m. $^{**}P < 0.01$. (**b**) Representative blot (top) and analysis of cortical soluble tau (by densitometry, bottom) normalized to α-tubulin (DM1A) in rat tissue 6 h after MCAO/reperfusion comparing L and UL hemispheres. Data are means ± s.e.m. $^{**}P < 0.01$. (**c**) Hippocampal tau and iron levels in mice after MCAO/reperfusion over time intervals indicated (two-way ANOVA with Sidak *post hoc* test). $n = 5$. Data are means ± s.e.m. $^{*/\#}P < 0.05$, $^{**}P < 0.01$, $^{***}P < 0.001$. $^{*/\#}$Reference is WT 0 h post reperfusion. *n* is indicated in the figure unless stated otherwise.

Chalfont, UK) was used for developing, and Fujifilm LAS-3000 (Tokyo, Japan) was used for visualization. Densitometry quantification of immunoreactive signals was performed by Image J (1.49 m; NIH), normalized to the relative amount of β-actin and expressed as percentage of the mean of the control group. The following antibodies were used in this study: antibody to APP (22C11, 1:1000, in-house); antibody to β-actin (1:5000; Sigma); antibody to ferroportin (fpn; MAP23, 1:1000, the kind gift of Dr TA Rouault); antibody to tau (1:2000; Dako); antibody to phosphorylated tau396 (1:1000; Invitrogen) and antibody to Cp (1:1000; Dako).

Rat sample preparation and western blot

Affected cortical tissues were homogenized in ice-cold lysis buffer containing 50 mM Tris-HCl (pH 7.6), 150 mM NaCl, 1% Triton X-100, 0.1% SDS, 1% deoxycholate, 1 mM EDTA and 1 mM $Na_3VO_4{\cdot}12H_2O$, 100 μg ml^{-1} phenylmethane sulfonyl fluoride (pH 7.5). Total protein concentration was determined by the BCA protein assay (Pierce). Aliquots of homogenate with equal protein concentration were separated by 10% (v v^{-1}) SDS-PAGE gel, and then transferred to nitrocellulose membrane. After blocking in 5% (w v^{-1}) nonfat milk for 1 h at room temperature, the membranes were then incubated with primary antibodies at 4 °C overnight. The blots were then incubated with anti-rabbit or anti-mouse IgG conjugated to IRDye (800CW) for 1 h at room temperature and visualized using the Odyssey Infrared Imaging System (Licor Biosciences, Lincoln, NE, USA). The antibodies used for rat samples were: tau-5 (1:1000; Millipore) and DM1A (1:2000; Abcam, Cambridge, UK).

Metal analysis

Mouse tissue metal content was measured as described previously.[11] Briefly, samples from each experimental condition were freeze dried, and then resuspended in 65% nitric acid (Suprapur; Merck, Darmstadt, Germany) overnight. The samples were then heated for 20 min at 90 °C, and the equivalent volume of hydrogen peroxide (30% Aristar, BDH) was added for a further 15 min incubation at 70 °C. The samples were diluted in double-distilled water and assayed by inductively coupled plasma mass spectrometer (Agilent 7700; Agilent Technologies, Santa Clara, CA, USA). Each sample was measured in triplicate and the concentrations determined from a standard curve and normalized to protein concentration.

Iron, copper and zinc concentrations in rat tissue were determined by flame atomic absorption spectroscopy. Briefly, brain tissue from each experimental condition was suspended in 65% nitric acid (ultraclean grade, 2 ml) and 70% perchloric acid (ultraclean grade, 0.25 ml). The samples were then heated for 30 min at 280 °C on a Hotplate (EH35B; Labtech, Hopkinton, MA, USA), and then triple-distilled water (5 ml) was added into the dried tissue for 15 min incubation at room temperature. The samples were then assayed by using flame atomic absorption spectrophotometer AA-240FS from Varian (Palo Alto, CA, USA). The concentrations determined from the standard curve were normalized to tissue wet weight.

Statistics

Statistical analysis was carried out in Prism 6 (GraphPad Software, La Jolla, CA, USA) and power calculations were performed using PASS 13 (trial version, NCSS Statistical Software, Kaysville, UT, USA) based on the variance of results in our previous publication[11] and in pilot experiments. Equivalence of variance between experimental groups was confirmed using Levene's test, when applicable. All tests were two tailed, with the level of significance set at 0.05. Specific tests used in each experiment are described in the text.

RESULTS

Reduction of tau precedes elevation of iron after MCAO/reperfusion

We examined a rat MCAO model of ischemic stroke and found the expected iron elevation in the lesioned hemisphere (+47%, $P = 0.003$, ratio paired *t*-test; Figure 1a) 6 h after reperfusion. Copper and zinc were unchanged (Supplementary Figures 1a and b). We hypothesized that in ischemic stroke tau may be involved in iron accumulation, and indeed found a marked reduction of tau (−5 to 5%, $P = 0.003$, ratio paired *t*-test; Figure 1b), concomitant with the significant elevation of iron in the lesioned hemisphere (Figure 1a). We explored whether these changes also occur in mice and found a reciprocal temporal relationship between changes in hippocampal tau and iron over 24 h post MCAO reperfusion (Figure 1c) without changes in copper or zinc (Supplementary Figures 1c and d), supporting a potential causal relationship between tau reduction and iron accumulation.

Age-dependent neuroprotection by tau suppression in experimental ischemic stroke

To test whether tau loss induced by MCAO has a causal role in neurotoxicity during reperfusion through iron accumulation, we tested the impact of the MCAO lesion on both 3-month- and 12-

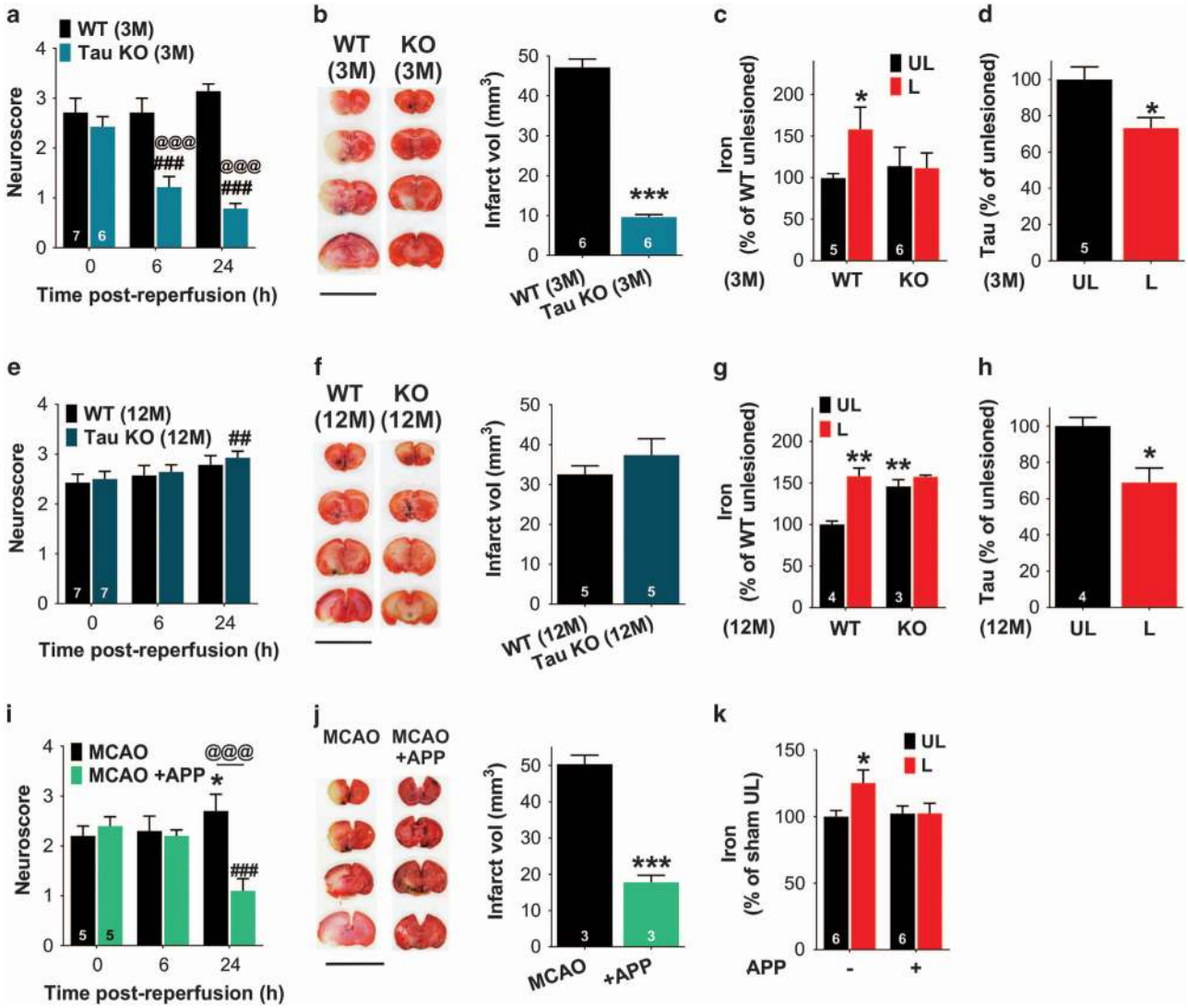

Figure 2. Age-dependent neuroprotection by tau suppression in experimental ischemic stroke. (**a** and **b**) Progressive neurological deficit and final infarct volumes after transient MCAO/reperfusion in 3-month-old WT and tau-knockout mice. Neurological scoring (higher numbers indicating more severe impairment) was performed at 0, 6 and 24 h after MCAO/reperfusion (**a**). Representative 2,3,5-tripenyltetrazolium chloride (TTC)-stained serial brain sections of mice 24 h after MCAO/reperfusion, where viable tissue stains red (**b**, left). Scale bar = 1 cm. Quantification of infarct volume (vol) indicated by TTC staining using Image J (**b**, right). (**c**) Hippocampal iron levels in 3-month-old WT and tau-knockout mice 6 h after MCAO/reperfusion, comparing L to UL hemispheres, normalized to protein. (**d**) Levels of hippocampal soluble tau normalized to β-actin in mice 6 h after MCAO/reperfusion comparing L to UL hemispheres. (**e** and **f**) Progressive neurological deficit and final infarct volumes after transient MCAO/reperfusion in 12-month-old WT and tau-knockout mice. Neurological scoring was performed at 0, 6 and 24 h after MCAO/reperfusion (**e**). Representative TTC-stained serial brain sections of mice 24 h after MCAO/reperfusion (**f**, left). Scale bar = 1 cm. Quantification of infarct volume (**f**, right). (**g**) Hippocampal iron levels in 12-month-old WT and tau-knockout mice, 6 h after MCAO/reperfusion comparing L to UL hemispheres, normalized to protein. (**h**) Hippocampal soluble tau normalized to β-actin in mice, 6 h after MCAO/reperfusion comparing L to UL hemispheres. (**I** and **j**) Intravenous APPec treatment immediately after reperfusion attenuated progressive neurological deficits (**i**) and final infarct volumes (**j**, right) after transient MCAO in 3-month-old C57/BL6 mice. Representative TTC-stained serial brain sections of mice 24 h after MCAO/reperfusion are shown in (**j**, left), scale bar = 1 cm. Data are means ± SEM. $^{*/\#}P < 0.05$, $^{**/@@}P < 0.01$, $^{***/\#\#\#/@@@}P < 0.001$. *Reference is WT unlesioned hemisphere (for **c**, **g**, **k**), or WT 0 h post reperfusion (for **a**, **e**, **i**). $^{\#R}$eference is tau-knockout mice 0 h post reperfusion. $^{@}$Reference is WT mice at matched time point post reperfusion. *n* is indicated in the figure unless stated otherwise.

month- old tau-knockout mice and their matched background controls (Bl6/129sv, wild-type (WT)), evaluating motor function, infarct size and metal levels after the lesion. We found that 3-month-old tau-knockout mice were markedly protected against MCAO-induced functional impairment indexed by neuroscore (6 h post reperfusion, $P < 0.001$ compared with WT; 24 h post reperfusion, $P < 0.001$ compared with WT; two-way repeated-measures ANOVA with Sidak *post hoc* test; Figure 2a), brain infarct volume measured by TTC staining (24 h post reperfusion, − 80%, $P < 0.001$, two-tailed *t*-test; Figure 2b) or CA1 neuronal loss by Nissl staining (for WT MCAO, − 66.1%, $P < 0.001$ compared with unlesioned; for Tau KO MCAO, +163.4%, $P < 0.001$ compared with WT MCAO lesioned; two-way repeated-measures ANOVA with Sidak *post hoc* test; Supplementary Figure 2). The neuroprotection occurred during reperfusion, as mice of both genotypes scored similarly at 0 h post reperfusion (Figure 2a), whereas mice with sham surgery consistently scored 0 points (data not shown). Real-time visualization of cerebral blood perfusion using Laser

Speckle Contrast Imager (PeriCam PSI System, Perimed, Järfälla, Sweden) revealed no differences in 3-month-old WT and tau-knockout mice during and after the MCAO procedure (Supplementary Figure 3). Neither differences in cerebral blood flow assayed by laser Doppler flow immediately after the occlusions nor differences in weight loss, heart rate or oxygen saturation were noted between the groups (Supplementary Figures 4a and e). The protection of 3-month-old tau-knockout mice from brain damage after MCAO with reperfusion recapitulated parallel independent findings using a different tau-knockout strain (Bi *et al.*, personal communication).

Consistent with the metal profile found in rats (Figures 1a and c and Supplementary Figure 1), iron was significantly elevated in the lesioned hemisphere of WT mice at 6 h post reperfusion (+58%, $P = 0.048$ compared with unlesioned hemisphere; two-way repeated-measures ANOVA with Sidak *post hoc* test; Figure 2c), and there were no changes in copper or zinc (Supplementary Figures 5a and b). As expected, unlesioned 3-month-old tau knockout brain had no increase in iron compared with WT (because iron accumulation commences at 7 months of age[11]), but unlike WT, ischemia–reperfusion induced no iron elevation (Figure 2c).

As with rats (Figure 1b), WT mice showed total tau suppression in the affected region 6 h post reperfusion (−27%, $P = 0.013$, ratio paired *t*-test; Figure 2d), but no change levels of pTau396 (Supplementary Figures 6a and b). We assessed that components of the iron efflux pathway, and found APP and Fpn, whose interaction is mediated by tau,[11] were unchanged after MCAO/reperfusion (Supplementary Figures 6a, c and d). Cp also facilitates the export of excess iron from the brain,[42] but unlike APP, not directly from neurons.[43] Post reperfusion, a significant elevation of Cp in both genotypes was observed (in WT mice, +82%, $P = 0.004$ compared with unlesioned hemisphere; in tau-knockout mice, +61%, $P = 0.013$; two-way repeated-measures ANOVA with Sidak *post hoc* test; Supplementary Figures 6a and e), consistent with a tau-independent homeostatic response.

The protection against reperfusion damage after MCAO conferred by tau knockout in 3-month-old mice was lost in the same strain at 12 months of age (Figures 2e and f) when brain iron overload is entrenched.[11] This could not be explained by vessel alterations as no differences were found in cerebral blood flow or physiological parameters between groups (Supplementary Figures 4f–i). While MCAO/reperfusion in 12-month-old WT mice induced brain iron accumulation after 6 h (+58%, $P = 0.006$ compared with unlesioned hemisphere; two-way repeated-measures ANOVA with Sidak *post hoc* test; Figure 2g), baseline levels of iron in the brain of tau-knockout mice were already similarly increased (+46%, $P = 0.002$ compared with WT unlesioned hemisphere, as expected;[11] $P = 0.635$ compared with lesioned hemisphere in tau-knockout mice), and no additional accumulation was found after MCAO/reperfusion. Copper and zinc levels were unaltered (Supplementary Figures 5c and d). Like younger WT, aged mice also had reduced tau levels after MCAO/reperfusion (−31%, $P = 0.042$, ratio paired *t*-test; Figure 2h), increased expression of Cp (in WT mice, +48%, $P = 0.032$ compared with unlesioned hemisphere; in tau-knockout mice, +75%, $P = 0.008$; two-way repeated-measures ANOVA with Sidak *post hoc* test; Supplementary Figure 6j) and no change in tau phosphorylation, APP or Fpn levels (Supplementary Figures 6f–i).

APP promotes iron export by stabilizing Fpn,[43–45] and tau loss causes toxic neuronal iron accumulation by abolishing APP trafficking to Fpn.[11] We previously showed in culture that adding soluble APP into the medium rescued the iron accumulation caused by ablation of tau.[11] We hypothesized that APP might cross the blood–brain barrier like Cp, which also promotes iron efflux by stabilizing surface Fpn, and which we had previously given parenterally to rescue toxic brain iron accumulation in a Parkinson's disease mouse model.[42] Therefore, we tested soluble amyloid precursor protein ectodomain (APPec) for neuroprotection in the ischemic stroke model. Indeed, intravenous injection of APPec after MCAO markedly prevented reperfusion injury, as evident from significantly improved neuroscores ($P < 0.001$ at 24 h compared with MCAO alone; two-way repeated-measures ANOVA with Sidak *post hoc* test; Figure 2i) and infarct volume 24 h post reperfusion (−65%, $P < 0.001$, two-tailed *t*-test; Figure 2j). APPec also prevented iron accumulation in the lesioned hemisphere after MCAO (for MCAO, +25.4%, $P = 0.013$ compared with unlesioned; for MCAO+APPec, +2.5%, $P = 0.999$ compared with unlesioned; two-way repeated-measures ANOVA with Sidak *post hoc* test; Figure 2k) without altering iron, copper or zinc content in the unlesioned hemisphere (Supplementary Figures 7a and b). These data indicate that ischemia–reperfusion perturbs the tau–APP axis of brain iron homeostasis.

Novel iron-targeted interventions for experimental ischemic stroke

We tested whether parenteral Cp treatment could also be salutary by negating brain iron accumulation in the ischemic stroke model. As this protein is highly selective in promoting iron export, and as it is available as a clinical infusion in some countries, we chose it to test whether interdicting the ischemia-mediated brain iron elevation in the acute phase (one dose) had enduring benefit. We found that peripheral Cp infusion delivered at the start of reperfusion significantly attenuated the functional impairments measured by Rotarod (day 1: $P < 0.001$; day 3: $P < 0.001$; day 7: $P < 0.001$; compared with MCAO; two-way repeated-measures ANOVA with Sidak *post hoc* test; Figure 3a) and neuroscore ($P < 0.001$ comparing two curves; two-way repeated-measures ANOVA with Sidak *post hoc* test; Figure 3b), and reduced infarct sizes 24 h later and maintained over the course of the study (−50% after 7 days, $P = 0.001$ compared with MCAO; one-way ANOVA with Tukey's *post hoc* test; Figure 3c). There is no progression of infarct volume for WT MCAO after 24 h ($P = 0.57$, one-way ANOVA with Tukey's *post hoc* test; Figure 3c), consistent with previous findings.[46]

Examined 24 h after infusion, Cp significantly prevented CA1 neuronal loss (for MCAO, −37.7%, $P < 0.001$ compared with unlesioned; for MCAO+Cp, −10.9%, $P = 0.015$ compared with unlesioned; +59.9%, $P < 0.001$ compared with MCAO lesioned; two-way repeated-measures ANOVA with Sidak *post hoc* test; Figure 3d), and suppressed ischemia-induced hippocampal iron elevation in the lesioned hemisphere (−48%, $P = 0.028$ compared with MCAO; one-way ANOVA with Tukey's *post hoc* test; Figure 3e). Cp treatment did not lower unlesioned brain iron (Supplementary Figure 8a), indicating that the treatment selectively suppresses the emergence of pathological iron accumulation, with no impact on copper and zinc (Supplementary Figures 8b and c). Similarly, rescue by Cp did not correct the hemisphere tau levels suppressed by ischemia (for MCAO alone, −39%, $P = 0.003$ vs unlesioned hemisphere; for MCAO+Cp, −29%, $P = 0.018$ vs unlesioned hemisphere; two-way repeated-measures ANOVA with Sidak *post hoc* test; Supplementary Figures 8d and e).

Intraperitoneal Cp treatment significantly increased both mouse brain Cp protein levels (+31.2%, $P = 0.009$; two-way repeated-measures ANOVA with Sidak *post hoc* test; Supplementary Figures 8d and f) and activity (+41%, $P = 0.037$ in transferrin assay; +20%, $P = 0.019$ in ferene S assay; two-way repeated-measures ANOVA with Sidak *post hoc* test; Supplementary Figures 8g and h), as reported previously.[42] As Cp was so effective at rescuing the stroke model, we were curious as to why the elevation of brain Cp induced acutely by the ischemia–reperfusion lesion (Supplementary Figures 6e, j and 8f) was insufficient to prevent the infarct. We found that the rise in hemispheric Cp protein induced by ischemia was not matched by increased oxidase activity (Supplementary Figures 8g and h). This indicates that while ischemia may induce a homeostatic increase in brain Cp

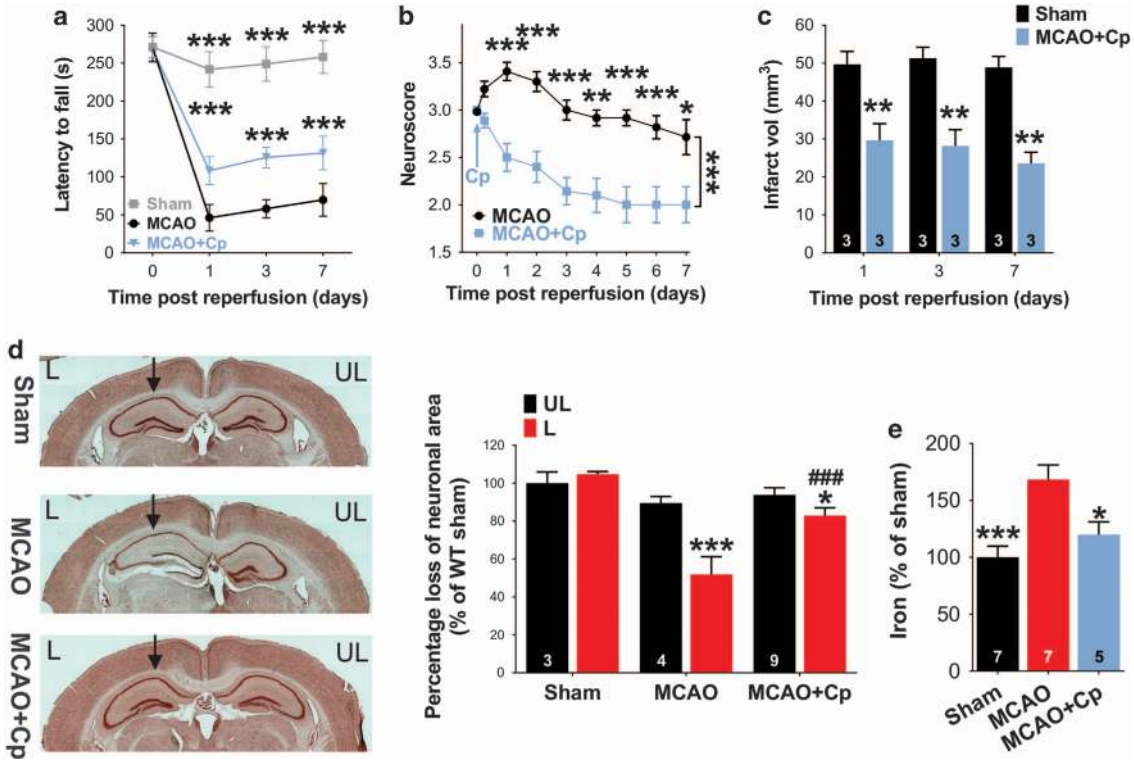

Figure 3. Facilitating iron export by Cp rescues ischemia–reperfusion injury. (**a–c**) Long-term effect of Cp treatment following transient MCAO in 3-month-old C57/BL6 mice, measured by rotarod (**a**), neuroscore (**b**) and infarct vol (**c**). $n = 6$ per group for (**a** and **b**). *$P < 0.05$; **$P < 0.01$; ***$P < 0.001$. *Reference is MCAO at matched time point or as indicated. (**d**) Cp treatment prevented hippocampal neuronal loss in mice with MCAO. Representative images (left) of the hippocampus from Sham-treated, MCAO and Cp post-treated MCAO mice, Nissl-stained 24 h after MCAO/reperfusion, comparing lesioned (L) to unlesioned (UL) hemispheres. Arrows show the region for quantification. Quantifications (right) of loss of neuronal area in CA1 region.. Data are means ± s.e.m. ***$P < 0.001$. *Reference is MCAO UL. (**f**) Hippocampal iron levels following transient MCAO in 3-month-old C57/BL6 mice, 6 h after reperfusion, were elevated compared to sham-lesioned hippocampal tissue, but intraperitoenal Cp treatment at reperfusion suppressed the elevation. Values are normalized to protein. Data are means ± s.e.m. *$P < 0.05$; ** $P < 0.01$. *Reference is MCAO. *n* is indicated in the figure unless stated otherwise.

production, the Cp is inactive, possibly because sufficient copper to enable the cuproenzyme activity does not reach the apoprotein. This would be consistent with the unchanged copper levels in ischemic brain (Supplementary Figure 8b). Indeed, substituting a Cp preparation that had been deactivated by removing copper (apo-Cp) abolished the neuroprotection seen with active Cp after MCAO/reperfusion (Supplementary Figure 8i), confirming that Cp electrochemical activity (to facilitate iron export) is crucial for its protective effect.

The involvement of ferroptosis in the ischemia–reperfusion toxicity

These findings unify previous findings of iron elevation in stroke with failure of Fpn-mediated iron export as a common pathway, but the molecular basis of toxicity is uncertain. Ferroptosis is a recently characterized, iron-dependent form of regulated non-apoptotic cell death.[47] Liproxstatin-1 is a potent and specific ferroptosis inhibitor, previously shown to limit ischemia–reperfusion damage in the liver.[48] To test whether the iron pool that exaggerates the stroke lesion fuels ferroptotic tissue loss, we treated 3-month-old mice after MCAO, commencing at early reperfusion, with liproxstatin-1 intranasally (acute treatment), as this route is known to bypass the blood–brain barrier. Liproxstatin-1 markedly attenuated MCAO-induced functional deficits, evidenced by Rotarod up to 7 days post treatment (day 1: $P < 0.001$; day 3: $P < 0.001$; day 7: $P < 0.001$; compared with MCAO; two-way repeated-measures ANOVA with Sidak *post hoc* test; Figure 4a), improved neuroscore ($P < 0.001$ comparing two curves; two-way repeated-measures ANOVA with Sidak *post hoc* test; Figure 4b), and reduced infarct volumes 14 days post reperfusion (−88%, $P < 0.001$, two-tailed *t*-test; Figure 4c), indicating a direct involvement of ferroptosis in ischemic stroke. Notably, liproxstatin-1 treatment alleviated MCAO-induced cognitive impairment, evidenced by improved ability to recognize novel objects in the motor-independent Novel Objective Recognition Test ($P = 0.027$, one-way ANOVA with Tukey's *post hoc* test; Figure 4d), and significantly enhanced performance in the Morris water maze ($P = 0.008$ comparing two curves; two-way repeated-measures ANOVA with Sidak *post hoc* test; Supplementary Figures 9a and b). No significant differences of swim speed were found between MCAO and MCAO with Lip-1 treatment group (for day 5, $P = 0.236$, two-way repeated-measures ANOVA with Sidak *post hoc* test; Supplementary Figure 9c). Ferroptotic inhibition during reperfusion prevented toxicity sooner (6 h) than APPec (24 h, Figure 2i) or Cp (24 h, Figure 3b) in 3-month-old WT mice, indicating that it could be a more effective treatment than interventions that facilitate iron efflux.

We further treated the MCAO mice 6 h after reperfusion, with the same dose of liproxstatin-1 (delayed treatment), to explore the possible translational value of ferroptosis inhibitors. Delayed liproxstatin-1 treatment still significantly prevented ongoing neuronal damage, but to a lesser degree, evidenced by improved neuroscore ($P = 0.019$ at 24 h compared with MCAO 24 h; $P < 0.001$ at 48 h compared with MCAO 48 h; two-way repeated-measures ANOVA with Sidak *post hoc* test; Figure 4e), and reduced infarct volume (−43%, $P < 0.001$, one-way ANOVA with Tukey's *post hoc* test; Figure 4f).

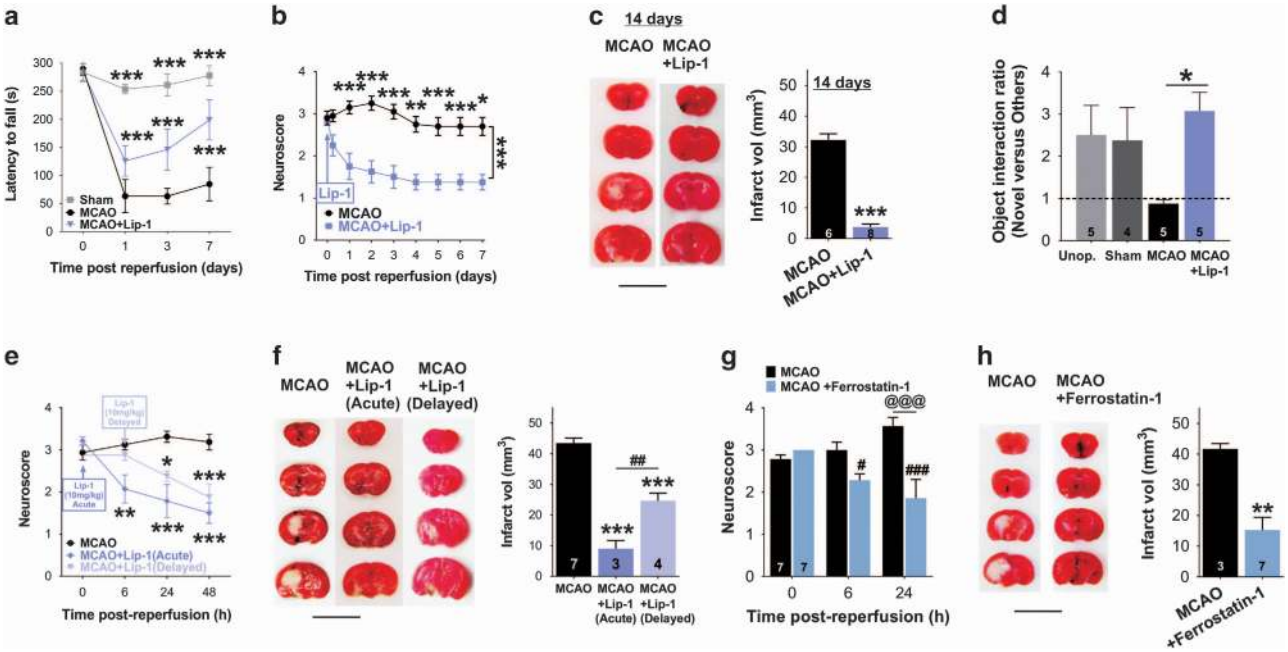

Figure 4. Targeting ferroptosis in ischemia–reperfusion injury. (**a–d**) Liproxstatin-1 treatment, given immediately after reperfusion, attenuated motor function decline measured by rotarod (**a**), progressive neurological deficits (**b**), $n = 8$, final infarct volumes (**c**, right) and cognitive function decline (**d**). Representative TTC-stained serial brain sections 24 h after MCAO/reperfusion are shown in (**c**, left), scale bar = 1 cm. (**e** and **f**) Delayed treatment (6 h after reperfusion) treatment with liproxstatin-1 attenuated progressive neurological deficits (**e**), n (MCAO) = 8, n (MCAO+Lip-1 acute) = 7, n (MCAO+Lip-1 delayed) = 4 and final infarct volumes (**f**, right). Representative TTC-stained serial brain sections of mice 24 h after MCAO/reperfusion are shown in (**f**, left), scale bar = 1 cm. (**g–h**) Ferrostatin-1 treatment immediately after reperfusion attenuated progressive neurological deficits (**g**) and final infarct volumes (**h**, right). Representative TTC-stained serial brain sections of mice 24 h after MCAO/reperfusion are shown in (**h**, left), scale bar = 1 cm. Data are means ± s.e.m. $*/^{@}P < 0.05$, $**/^{\#\#}/^{@@}P < 0.01$, $***/\#\#\#/^{@@@}P < 0.001$. *Reference is WT 0 h post reperfusion (**c**), MCAO (**c**, right; **f**, right; **h**, right), or as indicated. $^{\#}$Reference is treatment 0 h post reperfusion. $^{@}$Reference is MCAO mice at matched time point post reperfusion. n is indicated in the figure unless stated otherwise.

A second ferroptosis inhibitor, ferrostatin-1,[47] was used to confirm the involvement of ferroptosis in ischemia/reperfusion damage. Similar to liproxstatin-1, intranasal ferrostatin-1 delivered to 3-month-old Bl6/C57 mice after MCAO also attenuated neurological deficits ($P = 0.017$ at 6 h compared with 0 h post reperfusion; $P < 0.001$ at 24 h compared with 0 h post reperfusion; $P < 0.001$ at 24 h compared with MCAO 24 h; two-way repeated-measures ANOVA with Sidak *post hoc* test; Figure 4c) and infarct volumes 24 h post reperfusion (−63%, $P = 0.004$, two-tailed *t*-test; Figure 4d). Although ferroptosis is iron-dependent,[47] ferroptosis inhibitors do not target the iron levels in mouse brain, evidenced by no change in brain metal levels with the treatments (Supplementary Figures 10a–f). We also found that the rescue by ferroptosis inhibitors was dose-dependent, as a lower dose (5 mg kg^{-1} compared with 10 mg kg^{-1}) of either inhibitor did not rescue neurological deterioration after MCAO (Supplementary Figure 10g), while still being able to rescue infarct volume to a lesser degree (for liproxstatin-1, − 38%, $P = 0.002$ compared with MCAO; for ferrostatin-1, − 48%, $P < 0.001$ compared with MCAO; one-way ANOVA with Sidak *post hoc* test; Supplementary Figure 10h).

Lipoxygenase has been implicated in ferroptosis,[49] thus we tested ML351, a potent inhibitor of 15-lipoxygenase-1,[50] for its impact in ischemia–reperfusion-related brain damage. Intravenous injection of ML351 immediately after reperfusion was found to reduce neurological impairment ($P = 0.006$ at 24 h compared with 0 h post reperfusion; $P < 0.001$ at 24 h compared with MCAO 24 h; two-way repeated-measures ANOVA with Sidak *post hoc* test; Supplementary Figure 11a) and infarct volume (−40%, $P = 0.031$, two-tailed *t*-test; Supplementary Figure 11b) 24 h after the reperfusion, consistent with a previous report of the efficiency of ML351 in a permanent model of stroke.[50]

Rescue of MCAO in recalcitrant aged tau-knockout mice by iron-targeted interventions

The loss of protection against MCAO-induced damage in 12-month-old tau-knockout mice (Figures 2e and f) was caused by the accelerated increase in brain iron that occurs with aging with the loss of tau[11] (Figure 2g), because normalizing the iron elevation with Cp or preventing ferroptosis by liproxstatin-1 in the reperfusion phase reinstated the benefits of tau knockout as seen in 3-month-old animals (Figures 2a and b): reduced infarct volumes (for Cp, − 77%, $P < 0.001$; for Lip-1, − 55%, $P < 0.001$; compared with MCAO; two-way ANOVA with Sidak *post hoc* test; Figure 5a), and better function 24 h post reperfusion (for Cp, $P < 0.001$; for Lip-1, $P < 0.001$; compared with MCAO; two-way ANOVA with Sidak *post hoc* test; Figure 5b).

DISCUSSION

Our findings support a model (Figure 6) where ischemia–reperfusion injury acutely suppresses tau, a protein that normally facilitates iron export by trafficking APP to stabilize Fpn,[43–45] and so causes proferroptotic iron accumulation as a novel mechanism of injury in stroke. In young tau-knockout mice, brain iron homeostasis must be achieved by compensation from other non-tau-related systems. Therefore, ischemia–reperfusion does not generate a proferroptotic pool of iron in young tau-knockout mice (Figure 2c) because there is no tau for the ischemia to suppress, and so the infarct is attenuated. However, as the animal ages, homeostasis is lost prematurely in tau-knockout mice causing brain iron accumulation[11] (Figure 2g). Promoting iron efflux with Cp or APP (Figures 2 and 3) attenuates the infarct, consistent with previous results using chelation in normal animals.[15,20,22,23]

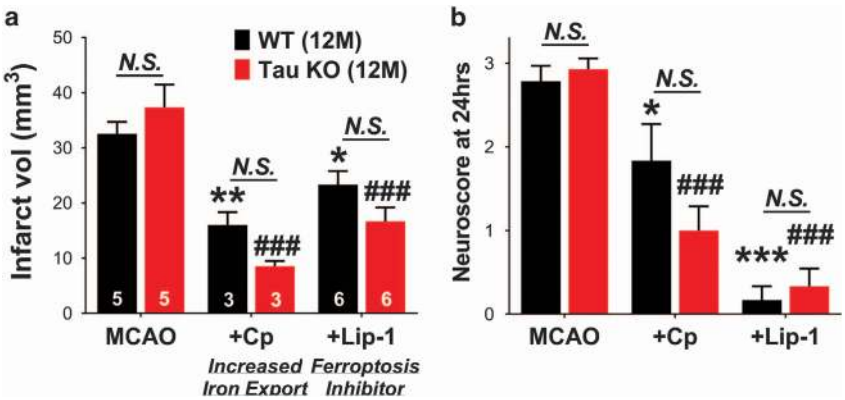

Figure 5. Tau reduction mediates iron-related neuronal damage in focal transient ischemia. Cp or Lip-1 treatment, given immediately after reperfusion, attenuated final infarct volumes (**a**) and neurological deficits (**b**) after transient MCAO in 12-month-old WT and tau-knockout mice, $n = 6$. Data are means ± s.e.m. $^{*}P < 0.05$, $^{**}P < 0.01$, $^{***/\#\#\#}P < 0.001$. *Reference is WT MCAO. #Reference is tau-knockout mice MCAO. *n* is indicated in the figure unless stated otherwise.

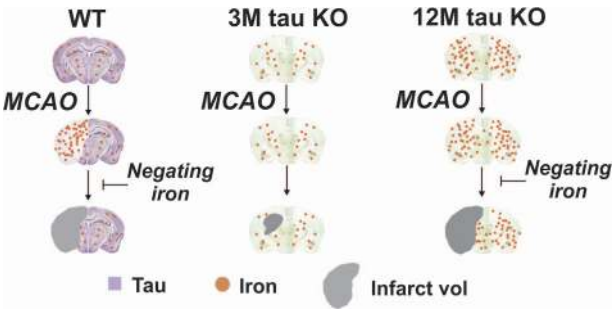

Figure 6. Schematic hypothesis. MCAO suppresses tau (purple stain), which leads to acute iron accumulation (brown dots), and exaggerates infarction (gray) upon reperfusion. When MCAO cannot reduce soluble tau protein (i.e. in 3-month-old tau-knockout mice), iron does not elevate, so the damage associated with reperfusion is more limited. Tau knockout causes brain iron to accumulate markedly after 7 months of age, so MCAO triggers exaggerated infarction in 12-month-old tau-knockout mice than the lesion in 3-month-old mice. Blocking MCAO-induced iron toxicity in 3-month-old WT or 12-month-old tau-knockout mice suppresses infarction to levels seen in 3-month-old tau-knockout mice.

Tau ablation is neuroprotective against ischemia–reperfusion injury, but only in young animals. Tau expression inhibits age-related brain iron accumulation,[11,27] and so exhibits antagonistic pleiotropy because while suppressing tau is neuroprotective in youth, it exaggerates neurotoxic iron accumulation with age. Thus, interdiction of the pathological iron pool is needed for tau ablation to be neuroprotective in 12-month-old animals (Figure 5). This neuroprotective effect of tau ablation has been shown, in work done in parallel to our own in a similar transient ischemia stroke model, to be through suppressing excitotoxic cell death (Bi *et al.*, personal communication).

Other programmed cell death pathways have been explored in the MCAO model, and recent work described the benefits of necroptosis inhibition by necrostatin-1.[51] However, necrostatin-1 was later identified to exhibit antiferroptotic properties.[48] While is not yet possible to exclude other forms of programmed cell death in the evolution of stroke,[52] ferroptosis is an attractive death mechanism for stroke because of the robust elevation of iron in the compromised tissue, and because previous approaches (e.g. blocking excitotoxicity) have failed to translate, possibly because they do not block ferroptosis. Furthermore, the penumbra has been customarily regarded as tissue that has undergone milder vascular compromise, and so can be rescued. However, ferroptosis originating from the infarct zone has the potential to cause or contribute to the penumbra as, in cell culture, it radiates as a contiguous wave of death that propagates in a synchronized non-cell-autonomous manner[53] in contrast to other forms of cell death, which are more stochastic.

As brain iron elevation occurs with normal human aging (reviewed Barnham and Bush[54]), as stroke becomes prevalent, our findings indicate that in order for tau-lowering strategies to be effective for human stroke, they may also need to unburden the brain of excess iron. These findings also underscore the need to study potential stroke interventions in older animals, at an age that better reflects the age of risk for stroke.[1] Many positive stroke interventions in younger animals have not translated into successful clinical trials,[55] but have not been studied in older animals. Our findings indicate that age-dependent iron elevation may confound the efficacy of a stroke intervention. These findings introduce the involvement of tau in mediating stroke-induced iron accumulation and outcome, as well as the therapeutic potential of ferroptotic inhibition in this injury.

CONFLICT OF INTEREST

Dr Adlard is a shareholder in and paid scientific consultant for Prana Biotechnology Ltd. Dr Bush is a shareholder in Prana Biotechnology Ltd, Cogstate Ltd, Mesoblast Ltd, NextVet Ltd, Brighton Biotech LLC and Cogstate Ltd, and a consultant for Collaborative Medicinal Development Pty Ltd.

ACKNOWLEDGMENTS

We thank Drs Mian Bi, Lars Ittner and Brian Stevens for technical assistance, and Drs Geoffrey Donnan, David Howells and Craig Rosenfeld for critical review of the manuscript. This work was supported by funds from the Australian Research Council, the National Health and Medical Research Council of Australia (NHMRC), the Cooperative Research Center for Mental Health, Alzheimer's Australia Dementia Research Foundation, National Natural Science Foundation of China (81722016, 81571236, 81271403, 81471304, 91632115) and the Fundamental Research Funds for the Central Universities (2015XJGH013, 2017SCU12042). P Lei is supported by the Recruitment Program of Global Young Experts of China.

AUTHOR CONTRIBUTIONS

PL and AIB conceived and raised funds for the study. RL raised funds for the study. Q-zT, PL, KAJ, X-lL, Z-yL, LR, SA, QW, PJC, PAA, RL and AIB designed and performed the experiments. KG and LP assisted with the experiments. PL, X-cW, Y-mL, RC, J-zW, RL and AIB supervised the experiments. Q-zT, PL and AIB

integrated the data and wrote the drafts of the manuscript. All authors edited the manuscript.

NOTES ADDED IN PROOF

Since the acceptance of this work, we learned that the protection of 3 month-old tau knockout mice from brain damage after MCAO with reperfusion recapitulated parallel independent findings using a different tau knockout strain, to be through suppressing excitotoxic cell death (Bi *et al*, Tau exacerbates excitotoxic brain damage in an animal model of stroke. Nature Communications, accepted, NCOMMS-17-18086).

REFERENCES

1 Krishnamurthi RV, Feigin VL, Forouzanfar MH, Mensah GA, Connor M, Bennett DA *et al.* Global and regional burden of first-ever ischaemic and haemorrhagic stroke during 1990–2010: findings from the Global Burden of Disease Study 2010. *Lancet Glob Health* 2013; **1**: e259–e281.
2 Langhorne P, Bernhardt J, Kwakkel G. Stroke rehabilitation. *Lancet* 2011; **377**: 1693–1702.
3 Yeo LL, Paliwal P, Teoh HL, Seet RC, Chan BP, Liang S *et al.* Timing of recanalization after intravenous thrombolysis and functional outcomes after acute ischemic stroke. *JAMA Neurol* 2013; **70**: 353–358.
4 Iadecola C, Anrather J. Stroke research at a crossroad: asking the brain for directions. *Nat Neurosci* 2011; **14**: 1363–1368.
5 Kikuchi K, Tanaka E, Murai Y, Tancharoen S. Clinical trials in acute ischemic stroke. *CNS Drugs* 2014; **28**: 929–938.
6 Foundation NS. *The Economic Impact of Stroke in Australia*, 2013.
7 DiNapoli VA, Huber JD, Houser K, Li X, Rosen CL. Early disruptions of the blood–brain barrier may contribute to exacerbated neuronal damage and prolonged functional recovery following stroke in aged rats. *Neurobiol Aging* 2008; **29**: 753–764.
8 Jin K, Mao X, Xie L, Greenberg RB, Peng B, Moore A *et al.* Delayed transplantation of human neural precursor cells improves outcome from focal cerebral ischemia in aged rats. *Aging Cell* 2010; **9**: 1076–1083.
9 Maynard CJ, Cappai R, Volitaskis I, Cherny RA, White AR, Beyreuther K *et al.* Overexpression of Alzheimer's disease amyloid-beta opposes the age-dependent elevations of brain copper and iron. *J Biol Chem* 2002; **277**: 44670–44676.
10 Maynard CJ, Cappai R, Volitakis I, Cherny RA, Masters CL, Li QX *et al.* Gender and genetic background effects on brain metal levels in APP transgenic and normal mice: implications for Alzheimer beta-amyloid pathology. *J Inorg Biochem* 2006; **100**: 952–962.
11 Lei P, Ayton S, Finkelstein DI, Spoerri L, Ciccotosto GD, Wright DK *et al.* Tau deficiency induces parkinsonism with dementia by impairing APP-mediated iron export. *Nat Med* 2012; **18**: 291–295.
12 Dietrich RB, Bradley WG Jr. Iron accumulation in the basal ganglia following severe ischemic–anoxic insults in children. *Radiology* 1988; **168**: 203–206.
13 Lipscomb DC, Gorman LG, Traystman RJ, Hurn PD. Low molecular weight iron in cerebral ischemic acidosis *in vivo*. *Stroke* 1998; **29**: 487–492; discussion 493.
14 Ding H, Yan CZ, Shi H, Zhao YS, Chang SY, Yu P *et al.* Hepcidin is involved in iron regulation in the ischemic brain. *PLoS ONE* 2011; **6**: e25324.
15 Park UJ, Lee YA, Won SM, Lee JH, Kang SH, Springer JE *et al.* Blood-derived iron mediates free radical production and neuronal death in the hippocampal CA1 area following transient forebrain ischemia in rat. *Acta Neuropathol* 2011; **121**: 459–473.
16 Fang KM, Cheng FC, Huang YL, Chung SY, Jian ZY, Lin MC. Trace element, antioxidant activity, and lipid peroxidation levels in brain cortex of gerbils after cerebral ischemic injury. *Biol Trace Elem Res* 2013; **152**: 66–74.
17 Kondo Y, Asanuma M, Nishibayashi S, Iwata E, Ogawa N. Late-onset lipid peroxidation and neuronal cell death following transient forebrain ischemia in rat brain. *Brain Res* 1997; **772**: 37–44.
18 Kondo Y, Ogawa N, Asanuma M, Ota Z, Mori A. Regional differences in late-onset iron deposition, ferritin, transferrin, astrocyte proliferation, and microglial activation after transient forebrain ischemia in rat brain. *J Cerebr Blood Flow Metab* 1995; **15**: 216–226.
19 Castellanos M, Puig N, Carbonell T, Castillo J, Martinez J, Rama R *et al.* Iron intake increases infarct volume after permanent middle cerebral artery occlusion in rats. *Brain Res* 2002; **952**: 1–6.
20 Patt A, Horesh IR, Berger EM, Harken AH, Repine JE. Iron depletion or chelation reduces ischemia/reperfusion-induced edema in gerbil brains. *J Pediatr Surg* 1990; **25**: 224–227; discussion 227–228.
21 Davis S, Helfaer MA, Traystman RJ, Hurn PD. Parallel antioxidant and anti-excitotoxic therapy improves outcome after incomplete global cerebral ischemia in dogs. *Stroke* 1997; **28**: 198–204; discussion 195–204.
22 Prass K, Ruscher K, Karsch M, Isaev N, Megow D, Priller J *et al.* Desferrioxamine induces delayed tolerance against cerebral ischemia *in vivo* and *in vitro*. *J Cerebr Blood Flow Metab* 2002; **22**: 520–525.
23 Hanson LR, Roeytenberg A, Martinez PM, Coppes VG, Sweet DC, Rao RJ *et al.* Intranasal deferoxamine provides increased brain exposure and significant protection in rat ischemic stroke. *J Pharmacol Exp Ther* 2009; **330**: 679–686.
24 Lei P, Ayton S, Finkelstein DI, Adlard PA, Masters CL, Bush AI. Tau protein: relevance to Parkinson's disease. *Int J Biochem Cell Biol* 2010; **42**: 1775–1778.
25 Ma QL, Zuo X, Yang F, Ubeda OJ, Gant DJ, Alaverdyan M *et al.* Loss of MAP function leads to hippocampal synapse loss and deficits in the Morris Water Maze with aging. *J Neurosci* 2014; **34**: 7124–7136.
26 Lei P, Ayton S, Moon S, Zhang Q, Volitakis I, Finkelstein DI *et al.* Motor and cognitive deficits in aged tau knockout mice in two background strains. *Mol Neurodegener* 2014; **9**: 29.
27 Lei P, Ayton S, Appukuttan AT, Volitakis I, Adlard PA, Finkelstein DI *et al.* Clioquinol rescues Parkinsonism and dementia phenotypes of the tau knockout mouse. *Neurobiol Dis* 2015; **81**: 168–175.
28 Lei P, Ayton S, Appukuttan AT, Moon S, Duce JA, Volitakis I *et al.* Lithium suppression of tau induces brain iron accumulation and neurodegeneration. *Mol Psychiatry* 2017; **22**: 396–406.
29 Roberson ED, Scearce-Levie K, Palop JJ, Yan F, Cheng IH, Wu T *et al.* Reducing endogenous tau ameliorates amyloid beta-induced deficits in an Alzheimer's disease mouse model. *Science* 2007; **316**: 750–754.
30 Ittner LM, Ke YD, Delerue F, Bi M, Gladbach A, van Eersel J *et al.* Dendritic function of tau mediates amyloid-beta toxicity in Alzheimer's disease mouse models. *Cell* 2010; **142**: 387–397.
31 Li X, Lei P, Tuo Q, Ayton S, Li QX, Moon S *et al.* Enduring elevations of hippocampal amyloid precursor protein and iron are features of beta-amyloid toxicity and are mediated by tau. *Neurotherapeutics* 2015; **12**: 862–873.
32 Dawson HN, Cantillana V, Jansen M, Wang HY, Vitek MP, Wilcock DM *et al.* Loss of tau elicits axonal degeneration in a mouse model of Alzheimer's disease. *Neuroscience* 2010; **169**: 516–531.
33 Dawson HN, Ferreira A, Eyster MV, Ghoshal N, Binder LI, Vitek MP. Inhibition of neuronal maturation in primary hippocampal neurons from tau deficient mice. *J Cell Sci* 2001; **114**(Part 6): 1179–1187.
34 Huuskonen MT, Tuo QZ, Loppi S, Dhungana H, Korhonen P, McInnes LE *et al.* The copper bis(thiosemicarbazone) complex CuII(atsm) is protective against cerebral ischemia through modulation of the inflammatory milieu. *Neurotherapeutics* 2017; **14**: 519–532.
35 Jackman K, Kunz A, Iadecola C. Modeling focal cerebral ischemia *in vivo*. *Methods Mol Biol* 2011; **793**: 195–209.
36 Alkayed NJ, Harukuni I, Kimes AS, London ED, Traystman RJ, Hurn PD. Gender-linked brain injury in experimental stroke. *Stroke* 1998; **29**: 159–165; discussion 166.
37 Bederson JB, Pitts LH, Tsuji M, Nishimura MC, Davis RL, Bartkowski H. Rat middle cerebral artery occlusion: evaluation of the model and development of a neurologic examination. *Stroke* 1986; **17**: 472–476.
38 Lin TN, He YY, Wu G, Khan M, Hsu CY. Effect of brain edema on infarct volume in a focal cerebral ischemia model in rats. *Stroke; a journal of cerebral circulation* 1993; **24**: 117–121.
39 Kang J, Lemaire HG, Unterbeck A, Salbaum JM, Masters CL, Grzeschik KH *et al.* The precursor of Alzheimer's disease amyloid A4 protein resembles a cell-surface receptor. *Nature* 1987; **325**: 733–736.
40 Aricescu AR, Lu W, Jones EY. A time- and cost-efficient system for high-level protein production in mammalian cells. *Acta Crystallogr D* 2006; **62**(Part 10): 1243–1250.
41 Wong BX, Ayton S, Lam LQ, Lei P, Adlard PA, Bush AI *et al.* A comparison of ceruloplasmin to biological polyanions in promoting the oxidation of Fe under physiologically relevant conditions. *Biochim Biophys Acta* 2014; **1840**: 3299–3310.
42 Ayton S, Lei P, Duce JA, Wong BX, Sedjahtera A, Adlard PA *et al.* Ceruloplasmin dysfunction and therapeutic potential for Parkinson disease. *Ann Neurol* 2013; **73**: 554–559.
43 Duce JA, Tsatsanis A, Cater MA, James SA, Robb E, Wikhe K *et al.* Iron-export ferroxidase activity of β-amyloid precursor protein is inhibited by zinc in Alzheimer's disease. *Cell* 2010; **142**: 857–867.
44 Wong BX, Tsatsanis A, Lim LQ, Adlard PA, Bush AI, Duce JA. Beta-Amyloid precursor protein does not possess ferroxidase activity but does stabilize the cell surface ferrous iron exporter ferroportin. *PLoS ONE* 2014; **9**: e114174.
45 McCarthy RC, Park YH, Kosman DJ. sAPP modulates iron efflux from brain microvascular endothelial cells by stabilizing the ferrous iron exporter ferroportin. *EMBO Rep* 2014; **15**: 809–815.
46 Liu F, Schafer DP, McCullough LD. TTC, fluoro-Jade B and NeuN staining confirm evolving phases of infarction induced by middle cerebral artery occlusion. *J Neurosci Methods* 2009; **179**: 1–8.
47 Dixon SJ, Lemberg KM, Lamprecht MR, Skouta R, Zaitsev EM, Gleason CE *et al.* Ferroptosis: an iron-dependent form of nonapoptotic cell death. *Cell* 2012; **149**: 1060–1072.

48 Friedmann Angeli JP, Schneider M, Proneth B, Tyurina YY, Tyurin VA, Hammond VJ *et al*. Inactivation of the ferroptosis regulator Gpx4 triggers acute renal failure in mice. *Nat Cell Biol* 2014; **16**: 1180–1191.
49 Conrad M, Angeli JP, Vandenabeele P, Stockwell BR. Regulated necrosis: disease relevance and therapeutic opportunities. *Nat Rev Drug Discov* 2016; **15**: 348–366.
50 Rai G, Joshi N, Jung JE, Liu Y, Schultz L, Yasgar A *et al*. Potent and selective inhibitors of human reticulocyte 12/15-lipoxygenase as anti-stroke therapies. *J Med Chem* 2014; **57**: 4035–4048.
51 Degterev A, Huang Z, Boyce M, Li Y, Jagtap P, Mizushima N *et al*. Chemical inhibitor of nonapoptotic cell death with therapeutic potential for ischemic brain injury. *Nat Chem Biol* 2005; **1**: 112–119.
52 Vanden Berghe T, Linkermann A, Jouan-Lanhouet S, Walczak H, Vandenabeele P. Regulated necrosis: the expanding network of non-apoptotic cell death pathways. *Nat Rev Mol Cell Biol* 2014; **15**: 135–147.
53 Linkermann A, Skouta R, Himmerkus N, Mulay SR, Dewitz C, De Zen F *et al*. Synchronized renal tubular cell death involves ferroptosis. *Proc Natl Acad Sci USA* 2014; **111**: 16836–16841.
54 Barnham KJ, Bush AI. Biological metals and metal-targeting compounds in major neurodegenerative diseases. *Chem Soc Rev* 2014; **43**: 6727–6749.
55 Fisher M, Feuerstein G, Howells DW, Hurn PD, Kent TA, Savitz SI *et al*. Update of the stroke therapy academic industry roundtable preclinical recommendations. *Stroke* 2009; **40**: 2244–2250.

Supplementary Information accompanies the paper on the Molecular Psychiatry website (http://www.nature.com/mp)